The use of ARMA to Generate Patterns of Extreme Loading on Long-Span Bridges

Michael J. Quilligan
Lecturer, School of Engineering, University of Limerick, Ireland

Eugene J. OBrien
Professor, School of Civil Engineering, University College Dublin, Ireland

ABSTRACT: For long-span bridges, the critical traffic loading condition is when vehicles are closely spaced during congestion events. While congestion can take various forms, most previous studies consider only a queue of vehicles with inter-vehicle gap distances based on constant values or those values taken from a statistical distribution. These models do not capture the trends present in recurrent traffic congestion where stop-and-go waves and oscillating congested traffic patterns can be present. For long-span bridges located in areas of heavy traffic these congestion events can occur daily, and this high frequency can increase the probability of a critical load case occurring. In this paper, an ARMA auto-regression moving average algorithm is used to generate future predictions of load effect from measured past effects. The concept is illustrated using traffic data collected from images taken with an Unmanned Aerial Vehicle (UAV) hovering over a highway subject to recurrent congestion. Vehicle positions and spacing data taken from the UAV are complemented by truck weight data from a nearby weigh-in-motion station. The ARMA model is shown to be an effective method of simulating congested event data. The methodology and findings have relevance for the development of a more accurate site-specific traffic load model for long-span bridges.

1. INTRODUCTION

In short to medium span bridges, the critical loading event involves an individual heavy vehicle or a small group in free flowing traffic. In contrast, the critical loading events for long-span structures are caused by congested traffic (Ivy et al. 1954; Flint & Neill Partnership, 1986; Buckland et al. 1980; Lutomirska and Nowak 2013). During congestion events, the gaps between vehicles reduce and the cumulative effect of many closely spaced vehicles produces the critical load event.

The accurate evaluation of traffic loading patterns on long-span bridges is however problematic. Data on inter-vehicle gaps, traditionally collected with inductive loop detectors, is not generally available for congested traffic as the loops are generally ineffective in stop-and-go conditions (Klein et al. 2006). Existing load models account for the variability of truck weights using Weigh-in-Motion (WIM) data. However, on a long-span bridge, the phenomenon of convoying is important, i.e., how many heavy vehicles are bunched together and what is the distance to the next convoy. For overturning moment in a bridge tower, vehicles can have an adverse or relieving effect. A key question then is the probability of a large bunch of closely spaced heavy vehicles followed by a lightly loaded section of traffic. WIM data does not include any of this information as WIM systems do not operate effectively in congested conditions. Conventional approaches, such as 'squashing' measured vehicle data by reducing the inter-vehicle gaps to a minimum, are highly ineffective and tend to be conservative. This results in excessive conservatism in new bridge designs and unnecessary interventions in existing bridges where characteristic maximum load effects have been over-estimated.

In this paper, a camera system in an Unmanned Aerial Vehicle (UAV) is proposed to collect data on inter-vehicle gaps and truck convoying patterns in congested traffic. Clearly a camera cannot detect vehicle weight but it has been found that weight estimates based on vehicle length is an effective means of calculating load effects.

This paper also proposes an ARMA model to simulate long-span bridge load effects from a limited supply of data. ARMA is a method of estimating future values from past data. An ARMA simulation is shown to generate a data set whose individual values are very different from those measured. However, the underlying trend, as it affects an extreme value calculation, is a very good match to the measurements.

2. DATA COLLECTION AND PROCESSING

The N7/M7 is a national primary route connecting Dublin to the south of Ireland. Prior to 2019 it was a three-lane carriageway in each direction for 20 km up to Junction 9 where the number of lanes reduced to two. With an Annual Average Daily Traffic (AADT) flow of approximately 105,000 vehicles, the lane drop at Junction 9 caused significant recurrent congestion during evening rush hour periods (Figure 1). The area was identified as being suitable for collecting congested traffic data from a bird's eye view using a UAV. A detailed description of the site and data collection and processing techniques are presented in Quilligan and OBrien (2020).

Traffic footage was collected using a DJI Phantom 4 Advanced quadrotor. Allowing for take-off, landing and a safe reserve of battery power, an average of 20 minutes traffic footage was collected in each flight. A limitation of the UAV used is that data collection is restricted to periods of no rain and wind speeds less than 35 km/h. The UAV hovered at a height of 120 m above ground and a distance of 30 m from the carriageway (Figure 2). At this height the road length captured was approximately 165 m, with a ground sampling distance of approximately 4.3 cm.

Figure 1: View of congested traffic forming due to lane drop at Junction 9.

Figure 2: Congested traffic observed from UAV.

The video footage was analysed using the cloud-based platform, DataFromSky (DFS). The system uses a deep learning convolution neural network algorithm to detect vehicles. Vehicle trajectories are filtered using vehicle kinematic models to ensure that small tracking errors do not result in sudden changes in positioning (Adamec et al. 2020).

The trajectory data output from DFS allows the density of the captured roadway length to be determined. Values are scaled from the captured road length to the standard 1 km distance which allows for density-time plots to be generated. To facilitate the determination of bridge load effects the data, recorded in a time reference, is transformed to a space reference using the equation:

$$dx_i = \overline{v_i} \times dT \qquad (1)$$

where dx_i is the space transform for frame i, $\overline{v_i}$ is the mean velocity for all vehicles in frame i (m/s) and dT is the sampling period (s). The effect of the transform is to rescale the X-axis, i.e. the axis is stretched when the mean velocity is high and squashed when the mean velocity is low.

Vehicle weights are accounted for by using Monte Carlo simulation to infer a 'typical' Gross Vehicle Weight (GVW) for each vehicle recorded in an image from a Cumulative Density Function (CDF) for that class of vehicle (Figure 3). The CDFs are created using data from a WIM site located 5.4 km from the test location.

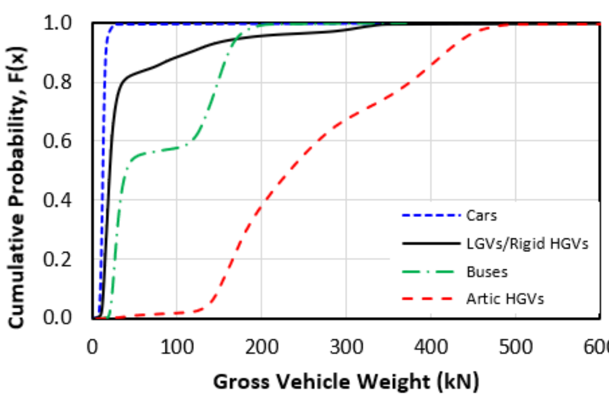

Figure 3: Cumulative Density Functions for vehicle weights for different vehicle classes.

Using the GVW data, the total weight of vehicles present can be determined for each frame of measured UAV data. Dividing the total weight of vehicles by the road length provides an Equivalent Uniformly Distributed Load (EUDL) for each frame. To simplify post processing of this data the X axis is broken into 10 segments and the EUDL per 10 m segment computed (Figure 4). This data then represents the load from a measured traffic stream and can be used to determine bridge load effects when it is traversed over an influence line.

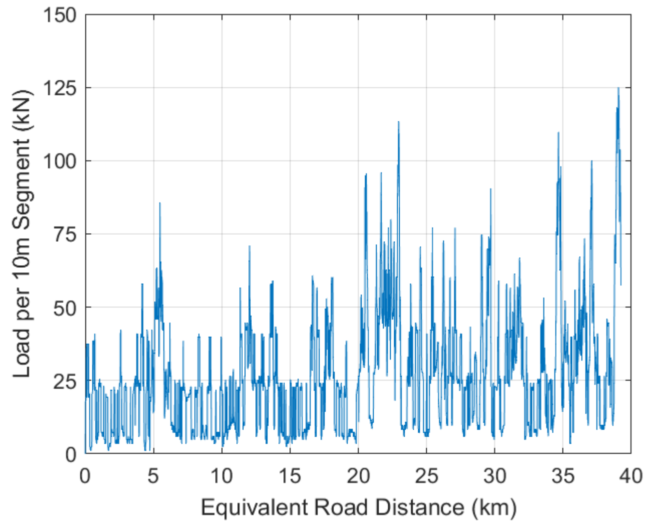

Figure 4: Load vs space for of 2 hours of combined UAV data.

3. CONGESTION MODELLING

3.1. Long-Span Load Effects

The effect of the traffic streams on long-span bridges is determined using an influence line over which the measured and simulated traffic streams can be passed. The Overturning Moment (OTM) in the tower of a suspension bridge is chosen for this study as it represents an important load effect where traffic can have an adverse or relieving effect, depending on its location on the structure. The OTM influence line used is illustrated in Figure 5 and is based on that of the Golden Gate (Enright et al. 2013) and Forth Road bridges. OTMs are positive for vehicles in the first side-span, negative for vehicles in the main-span and assumed to be negligible for vehicles in the far side-span. Lane 2 (slow) data is only used for this study as the measured data has a higher percentage of HGVs and there is therefore a greater load intensity in this lane.

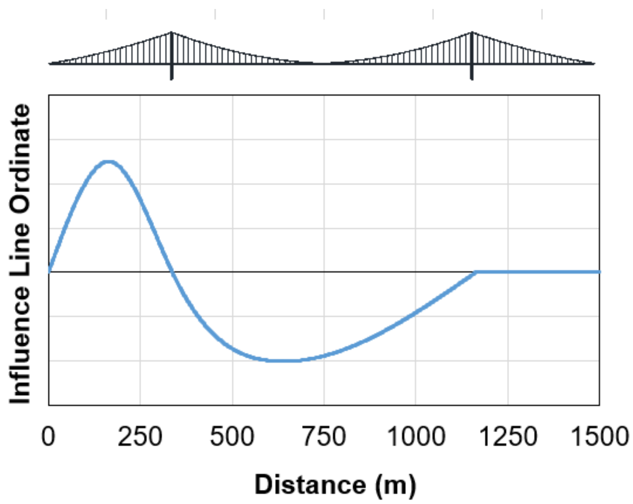

Figure 5: Influence line for tower Overturning Moment in suspension bridge of total length 1,500 m.

3.2. Conventional 'Squashed' Traffic Model

In many previous studies traffic data collected under free flowing conditions has been used to create a congested traffic stream by 'squashing' the gaps between following vehicles. To simulate full stop events, the bumper-to-bumper gap between vehicles has typically been set to 1.5 m (approximately equivalent to a 5.0 m axle-to-axle distance) by various studies (Ivy et al. 1954; ASCE 1981; Prat 2001; Hendy et al. 2015; Micu et al. 2018). To simulate the moving congestion present in recurrent congestion conditions, larger gap values have been used, some constant and some based on statistical distributions (Koshini 1985; Vrouwenvelder and Waarts 1993; Bailey 1996; Lutomirska and Nowak 2013).

For this study a conventional 'squashed' traffic model is used and the resultant load effects are compared to those from measured and simulated ARMA traffic streams. The squashing traffic model takes the vehicle class and arrival sequence data directly from the UAV-measured dataset. As this data does not have values for vehicle length, data from a nearby WIM station is used to create a probability density function of vehicle lengths for each vehicle class. A 'typical' length for each vehicle in the traffic stream is then generated using Monte Carlo simulation from the relevant distribution. A constant bumper-to-bumper gap of 4.5 m is used which is representative of the values adopted in the above referenced studies for slow moving congestion.

3.3. ARMA Model

As noted above, the measured UAV data is limited in its duration. Collection of additional data is restricted by the need to manually operate the UAV during congestion events and by certain weather conditions which prevent the flying of the UAV. As such a model that simulates additional data based on the trends present within the measured data is required.

Time series analysis is widely used as a data forecasting technique in many disciplines. An ARMA model combines auto-regressive (AR) and moving average (MA) functions to extract relevant information from a stationary time series, and can obtain effective predictions using limited historical data (Wang et al. 2020). Box et al. (1970) developed the concept of the ARMA model, proposing three parts to the process: model selection, parameter estimation and model testing. For a stationary time series $\{x_t\}$, the ARMA(p,q) model can be written as:

$$x_t = c + \sum_{i=1}^{p} \phi_i \, x_{t-1} + \sum_{j=1}^{q} \theta_j \, \varepsilon_{t-j} + \varepsilon_t \qquad (2)$$

where c is a constant, ϕ_i is the autoregressive parameter, p is the autoregressive order, θ_j is the moving average parameter, q is the moving average order and ε_t is white Gaussian noise with zero mean and constant variance.

While a preliminary order determination is undertaken by inspection of the truncation and tailing characteristics of the autocorrelation and partial autocorrelation coefficients, the Akaike Information Criterion (AIC) method is used to determine the appropriate orders of the model by studying a range of combinations. The AIC evaluates how well a model fits the data it was generated from. The best-fit model, indicated by the minimum AIC (Akaike 1974), is the one that uses the fewest possible independent variables to explain the greatest amount of variation, and is defined as:

$$AIC = 2K - 2logL \quad (3)$$

where K is the number of model parameters and L is the likelihood estimate, a measure of model fit.

The model is verified by checking whether the residual sequence of the fitted model is a white noise sequence. The resultant ARMA model can then be used to simulate new traffic streams which can be used to determine long-span load effects.

4. RESULTS

The sample of load data presented in Figure 4 is used in this study to determine OTMs in the tower of a 1,500 m suspension bridge under measured, conventional squashed and simulated ARMA traffic streams.

4.1. Conventional 'Squashed' Traffic Model

The tower OTM from the measured and conventional squashed traffic streams are illustrated in Figure 6. While there are similarities in the load effect curves from the measured and squashed traffic streams, there are some significant differences. A peak positive moment of +1.17 MNm is recorded under the measured stream, compared to +0.15 MNm under the squashed stream. The effect of having high density traffic on the first side-span combined with light free flowing traffic on the relieving main span is not captured by the squashed model, i.e. loading squashed traffic on both positive and negative sides of the full influence line results in a relieving effect which underestimates the maximum positive bending moment.

A fully bounded solution using the squashed traffic stream is possible if the relieving sections from the influence lines are removed, a process often adopted in industry practice. The load effect from these simulations is also illustrated in Figure 6. This model produces a series of extreme positive and negative OTMs, with a peak positive moment of +2.28 MNm recorded, which is approximately double the peak measured value.

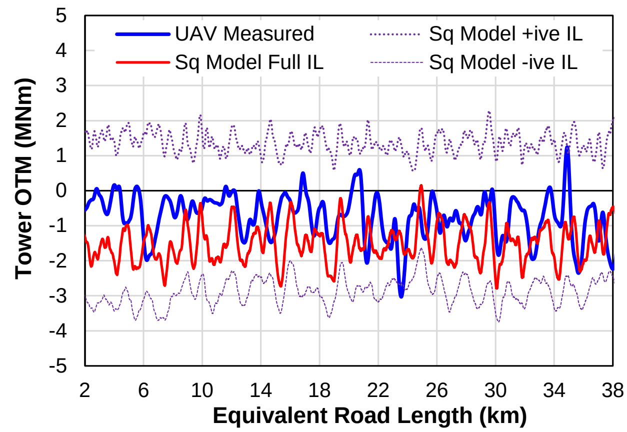

Figure 6: Tower OTM under measured and conventional 'squashed' traffic streams.

While the squashed traffic streams presented here are simplified, they highlight how conventional squashed gap models do not adequately represent patterns of load effects produced by the measured traffic congestion.

4.2. ARMA Model

ARMA models for a range of autoregressive and moving average orders are created and their resultant AIC values are presented in Table 1.

Table 1: AIC values for different p and q orders.

	p value				
q value	*0*	*1*	*2*	*3*	*4*
0		*30,492*	*30,491*	*30,492*	*30,794*
1	*36,483*	*30,490*	*30,492*	*30,493*	*30,495*
2	*34,170*	*30,492*	*30,493*	*30,497*	*30,496*
3	*32,987*	*30,494*	*30,495*	*30,496*	*30,491*
4	*32,228*	*30,495*	*30,497*	*30,497*	*30,495*

It is evident that the many of the AIC values are of a similar magnitude, with the lowest value for the ARMA(1,1) model. Figure 7 presents a plot of the standard residuals for this model compared to the measured data. The plot indicates that the model is a good fit as it corresponds to a white noise sequence with zero mean.

Table 2 presents the key parameters for this first order ARMA(1,1) model.

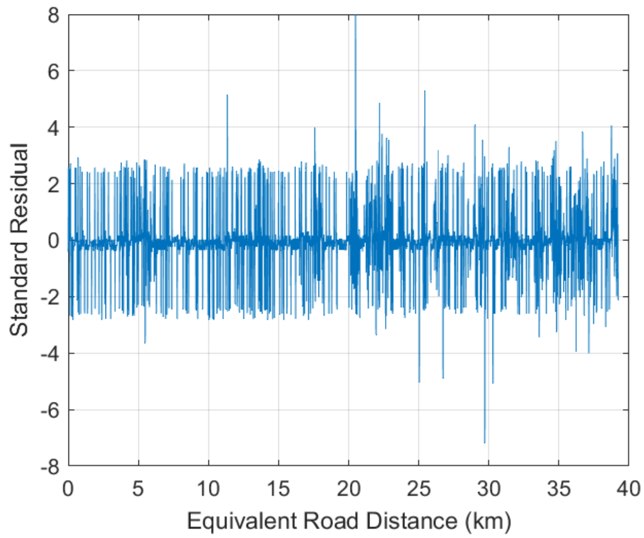

Figure 7: Standard residuals from ARMA(1,1) model.

Table 2: ARMA(1,1) model parameters.

Parameter	***Value***
Constant, c	*1.354*
Autoregressive parameter, ϕ	*0.950*
Moving Average parameter, θ	*-0.031*
Variance	*42.82*

Figure 8 illustrates the tower OTM under the measured and five simulated ARMA traffic streams. Visual comparison of the measured and ARMA load effects is difficult. However it is evident that there are similar ranges and frequencies of peaks and troughs.

Block maximum values are often plotted when calculating characteristic maximum load effects to determine the trend of increasing load effect with reducing probability. This trend has a significant influence on the calculated characteristic maximum, and is a key feature in extreme value data.

Figure 9 illustrates maximum values taken from 1 km blocks of measured and simulated load effects, plotted on Gumbel probability paper. It is evident that the ARMA model captures the nature of the measured data from these plots, with a similar slope, although the mean is slightly higher.

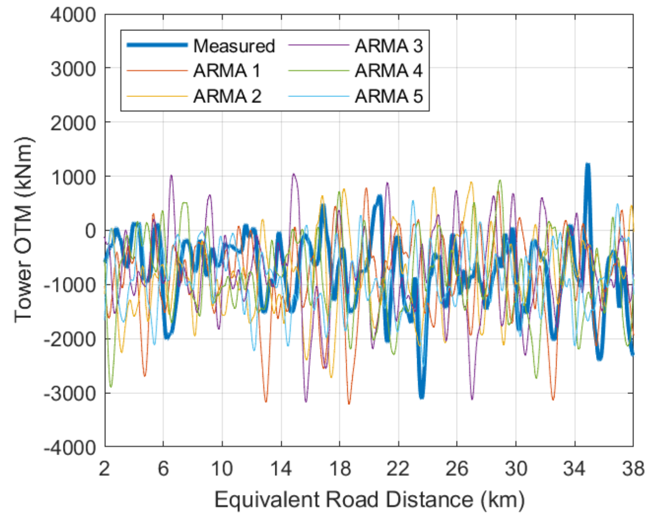

Figure 8: Tower OTM under measured and simulated ARMA traffic.

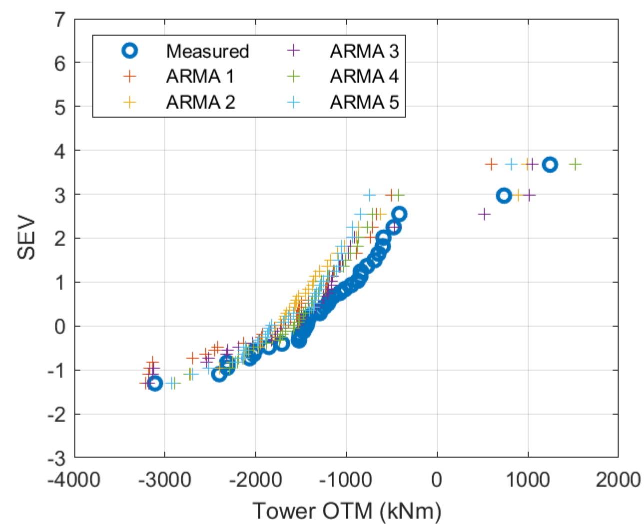

Figure 9: Gumbel probability paper plot of 1 km block maximum values for measured and ARMA traffic streams.

To allow a comparison with the load effect from conventional squashed traffic stream, 1 km block maxima are taken from the upper and lower bound curves in Figure 6 above, and are presented in Figure 10. The slopes and offsets of the block maxima values from the squashed traffic streams are significantly different to those derived from the measured and ARMA streams.

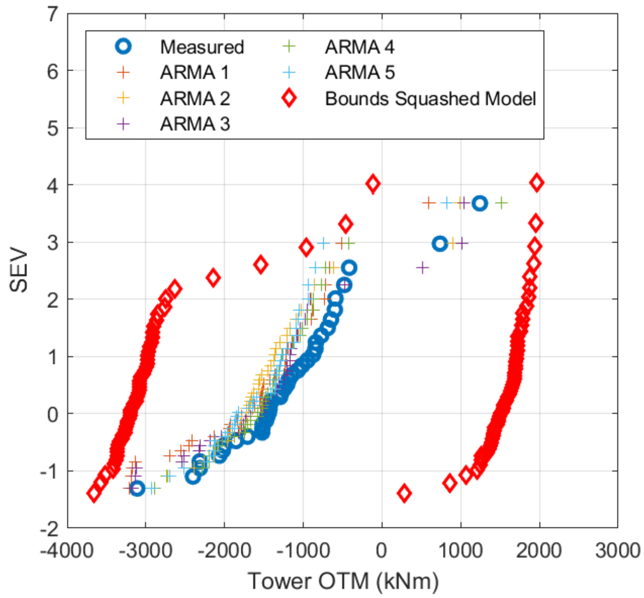

Figure 10: Gumbel probability paper plot of 1 km block maxima values for measured, conventional squashed and ARMA traffic streams.

Using the load effect data from the squashed traffic streams to extrapolate to a given return period would lead to inaccurate values for both positive and negative OTM. This data clearly indicates that the adoption of a conventional squashed traffic model does adequately represent the features present in the measured traffic data and the resultant load effects.

5. CONCLUSIONS

This paper investigates the novel use of an ARMA model to generate patterns of recurrent congestion on long-span bridges based on measured data from a UAV. For long-span bridges located in areas of high traffic these congestion events can occur daily, and this high frequency can increase the probability of a critical load case occurring.

The developed ARMA model is shown to capture the trends present in measured data and the resultant load effects have a representative spread of results when compared to those from the measured data.

It is shown that the use of a conventional 'squashed' traffic model to extrapolate load effect data to a given return period could lead to inaccurate non-conservative values. The ARMA model on the other hand demonstrates good potential for the calculation of site specific characteristic maximum load effects on long-span bridges.

6. REFERENCES

Adamec, V., Herman, D., Schullerova, B., and Urbanek, M., Modelling of Traffic Load by the DataFromSky System in the Smart City Concept, in Smart Governance for Cities: Perspectives and Experiences, N.V.M. Lopes, Editor. 2020, Springer Nature: Switzerland. p. 135-152.

Akaike, H. (1974) 'A new look at the statistical model identification', IEEE Transactions on Automatic Control, 19, 716–723, available: http://dx.doi.org/10.1109/TAC.1974.1100705.

ASCE (1981) 'Committee on Loads and Forces on Bridges - Recommended Design Loads for Bridges', ASCE Journal of the Structural Division, 107(7), 1161-1213.

Bailey, S.F. (1996) Basic Principles and Load Models for the Structural Safety Evaluation of Existing Bridges, unpublished thesis (PhD), Ecole Polytechnique Fédérale de Lausanne.

Box, G.E., Jenkins, G.M. and Reinsel, G.C. (1996) Time series analysis: forecasting and control, New Jersey: Prentice Hall International.

Buckland, P.G., McBryde, J.P., Zidek, J.V., and Navin, F.P.D., Proposed Vehicle Loading of Long-Span Bridges. Journal of the Structural Division, 1980. 106(4): p. 915-932.

Enright, B., Carey, C. and Caprani, C.C. (2013) 'Microsimulation evaluation of Eurocode load model for American long-span bridges', Journal of Bridge Engineering, 18(12), 1252-1260.

Flint & Neill Partnership, Interim design standard: long span bridge loading. 1986: Crowthorne.

Ivy, R., Lin, T., Mitchell, S., Raab, N., Richey, V. and Scheffey, C. (1954) 'Live loading for long-span highway bridges', American Society of Civil Engineers Transactions.

Klein, L.A., Mills, M.K., and Gibson, D.R., Traffic detector handbook: Volume I. 2006, Turner-Fairbank Highway Research Center.

Koshini, I. (1985) 'Traffic load measurement and probabilistic modelling for structural design of urban expressways', in Konishi, I., Ang, A. H.-S. and Shinozuka, M., eds., 4th International

Conference on Structural Society, ICOSSAR'85, Kobe, Japan.

Lutomirska, M. and Nowak, A.S. (2013) 'Site-specific live load and extreme live load models for long span bridges', in Safety, Reliability, Risk and Life-Cycle Performance of Structures and Infrastructures - Proceedings of the 11th International Conference on Structural Safety and Reliability, ICOSSAR 2013, 3741-3747.

Micu, E.A., OBrien, E.J., Malekjafarian, A. and Quilligan, M. (2018) 'Estimation of Extreme Load Effects on Long-Span Bridges Using Traffic Image Data', The Baltic Journal of Road and Bridge Engineering, 13(4), 429-446, available: http://dx.doi.org/10.7250/bjrbe.2018-13.427.

Prat, M. (2001) 'Traffic load models for bridge design: recent developments and research', Progress in Structural Engineering and Materials, 3(4), 326–334, available: http://dx.doi.org/10.1002/pse.91).

Vrouwenvelder, A.C.W.M. and Waarts, P.H. (1993) 'Traffic Loads on Bridges', Structural Engineering International, 3(3), 169-177.

Wang, Y., Wang, D. and Tang, Y., 2020. Clustered hybrid wind power prediction model based on ARMA, PSO-SVM, and clustering methods. IEEE Access, 8, pp.17071-17079.